GEOMETRIC CALIBRATION OF THIRD-GENERATION COMPUTED TOMOGRAPHY SCANNERS FROM SCANS OF UNKNOWN OBJECTS USING COMPLEMENTARY RAYS

Kevin M. Holt

Varian Medical Systems, Lincolnshire IL, USA

ABSTRACT

To achieve good image quality for computed tomography scans, it is important to accurately know the geometrical relationship between the x-ray source, detector, and axis of rotation. Conventional geometric calibration algorithms generally require particular calibration phantoms, such as a small pin or wire, which may not be practical for all scanner types, particularly for large industrial scanners. This paper presents an alternative framework to calibrate system geometry from scans of arbitrary objects, without prior knowledge of the object's form. This lessens physical construction requirements, and permits post-scan geometric calibration from any arbitrary scan data. Experimental results show that central ray calibration using this approach can give results accurate to 0.01 channels for low-noise conditions, or 0.1-0.45 channels under higher noise levels.

Index Terms— Tomography, Calibration

1. INTRODUCTION

Computed Tomography (CT) scanning is a technique wherein one projects X-rays through an object from many different angles, then processes the resulting projection data to form an image of the local linear attenuation coefficients in a cross-section through the object. Such images can be used to see structure, density variations, and changes in material composition; hence CT has become a popular tool for medical diagnosis, industrial non-destructive testing and reverse engineering, and security inspection. Currently, the most popular CT configuration is so-called *third generation* CT, shown in Figure 1, where the source and detector are fixed with respect to each other, rotating relative to the object under study. The relative motion may be performed by rotating the source and the detector in tandem, as with typical medical geometries, or by rotating the object, as with typical industrial geometries. Slice location is adjusted by sliding along the Z-axis (parallel to the rotation axis), which for medical geometries is typically horizontal, and for industrial geometries is typically vertical – this motion is relative and may be performed by sliding the object, or by sliding the source and detector in unison.

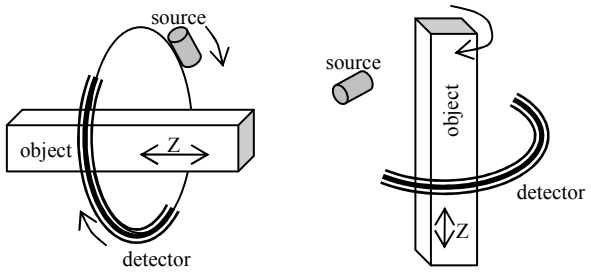

(a) Typical Medical Geometry (b) Typical Industrial Geometry

Fig. 1. Two types of third-generation scanners

For proper CT reconstruction, especially when the end goal is dimensional measurement, it is important to accurately know the relative position of each detector channel with respect to the x-ray source and rotation axis. For medical geometries, the rotation axis is fixed, and alignment is generally fairly stable over time. For industrial geometries, however, alignment may easily change as a function of Z. Though one can calibrate alignment as a function of Z, when the range of Z positions is large the results can be inaccurate when using relatively flimsy calibration objects such as pins or wires, which are typically required by conventional calibration algorithms. Further, particularly heavy objects may cause the scanner to flex, causing alignment to change as a function of the scan object.

In this paper, a framework is proposed in which one can measure alignment from scans of arbitrary objects by maximizing the redundancy in complementary rays. This allows the use of large rigid calibration objects which are stable over large ranges of Z, and whose weight distribution matches the object to be scanned. Furthermore, one can calibrate from the same projection data that will be reconstructed, eliminating both the need for the operator to perform an extra calibration step, as well as the risk of the alignment changing between the calibration and object scan. Section 2 provides an overview of geometric calibration, Section 3 describes the proposed framework, and Section 4 gives experimental results validating the proposed approach.

2. GEOMETRIC CALIBRATION

Figure 2 shows a third-generation CT geometry. There are N detector channels, numbered 0 to $N-1$. The *central ray*

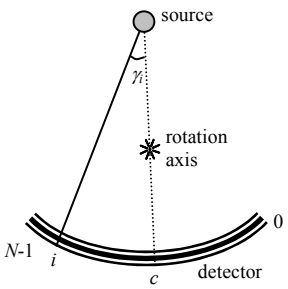

Fig. 2. Scanner Geometry

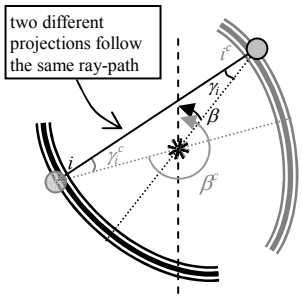

Fig. 3. Complementary Rays

(also referred to as *iso-ray*), is defined as the ray that passes from the source through the rotation axis; it intersects the detector at channel c (called the central ray value), which in general is non-integer. For an arbitrary channel number i, let γ_i be its *channel angle*, defined as the angle between the central ray and the ray from the source to that channel.

To perform geometric calibration, we must first parameterize the geometry – specifically, let us parameterize the angles γ_i based on the known construction of the detector, and denote the set of unknown parameters as Θ.

One construction is equiangular detectors, where channels are spaced with constant angular pitch $\Delta\gamma$ along an arc focused on the source, and the angles are modeled as:

$$\gamma_i = \Delta\gamma \times (i - c) \,. \tag{1}$$

Another important case is equilinear detectors, where channels are equally spaced along a flat line perpendicular to the central ray, and the channel angles are modeled as

$$\gamma_i = \tan^{-1}\left(\Delta\gamma \times (i - c)\right), \tag{2}$$

where angular pitch is no longer constant, but $\Delta\gamma$ is the local angular pitch, in radians, about the central ray.

For either of these equally spaced detectors, let's use the term "*c-ray calibration*" to denote that $\Delta\gamma$ is known ahead of time, and our goal is to measure

$$\Theta = \{c\} \,. \tag{3}$$

Similarly, let's use the term "*cray+pitch calibration*" to denote that neither c nor $\Delta\gamma$ is known, and we measure

$$\Theta = \{c, \Delta\gamma\}, \tag{4}$$

Though we focus on c-ray and c-ray+pitch calibration in this paper, the results may be straightforwardly extended to other geometric types. For example, full angular calibration may be performed by using

$$\Theta = \{\gamma_i\}_{i=0}^{N-1} \,. \tag{5}$$

Additionally, detectors comprised of discrete modules in a polygonal or tiled configuration may be addressed by adding a position parameter for each module, or by parameterizing the gaps between modules.

3. CALIBRATION FROM COMPLEMENTARY RAYS

This section provides a general approach for finding any Θ from projection data of an arbitrary object. The basic idea is to imagine a number of different hypothetical geometries, calculate what patterns of redundancy we would expect to see in the data for each geometry, then select the geometry whose expected redundancy best matches the measured data.

Redundancy in complementary rays is well-known and commonly exploited, such as in [1]. Let β be the rotation angle of the object relative to the source and detector. As the object rotates, data is acquired for a large number of different β values, perhaps covering exactly 360°. One can see from Figure 3 that the path through the object from the source to channel i at position β should be identical to the path from the source to some other channel i^c at some second position β^c, where

$$\gamma_i = -\gamma_{i^c} \tag{6}$$

and

$$\beta + \gamma_i \equiv \beta^c + \gamma_{i^c} + \pi \tag{7}$$

where "$\equiv$" means equal, modulus 2π. We can rewrite (7) as

$$\beta^c \equiv \beta + 2\gamma_i + \pi \,. \tag{8}$$

Now let us denote our logged input projection data, after standard corrections and normalizations (see [2] section 7.5.1), by $P(i,k)$ where k is view number. Then for some Θ, let us define the complementary projection set as

$$Q_\Theta(i,k) \triangleq P\left(\gamma^{-1}(-\gamma_i), \beta^{-1}\left(\beta_k + 2\gamma_i + \pi\right)\right) \tag{9}$$

where the inverse equations $\gamma^{-1}(\cdot)$ and $\beta^{-1}(\cdot)$ represent the calculation of channel number from channel angle, and view number from rotation angle, respectively. In general, both inverse equations produce non-integer indices, so "$\triangleq$" indicates that an interpolation step is required to produce Q from P. This could be, for example, bilinear or cubic spline interpolation, but in practice, truncated sinc interpolation is far more robust to noise, for reasons described in [3]. Note that both the forward and inverse γ and β calculations depend on Θ, hence its appearance as a subscript on Q.

If Θ accurately describes the scanner geometry, then the X-ray path covered in a datum $P(i,k)$ should be identical to the X-ray path covered by $Q_\Theta(i,k)$. Thus, we expect that for the true value of Θ, then

$$P(i,k) \approx Q_\Theta(i,k) \tag{10}$$

Furthermore, since there is a one-to-one mapping between projection data and underlying images, and we know that the underlying image is the same in both P and Q, then as long as the underlying image is strong compared to the noise level, we expect (10) to hold if and *only* if Θ closely describes the true geometry during the acquisition of P.

Due to noise and differences in scatter, beam shape, detector response, etc., the equality in (10) will in general not be exact. Therefore, calibration is performed by minimizing some difference measure D,

$$\Theta^* = \arg\min_\Theta D\left(P; Q_\Theta\right) \,. \tag{11}$$

This is in essence a registration problem, and suitable choices for D include standard distance measures such as

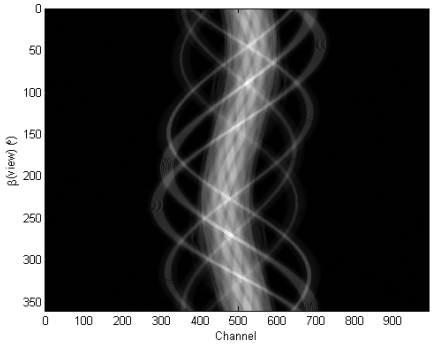

Fig. 4. Measured sinogram

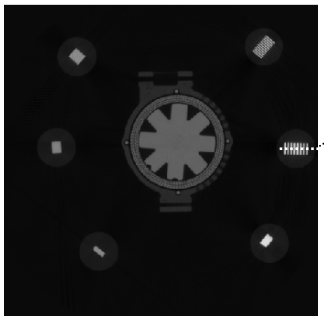

Fig. 6. Reconstruction of Fig 4 using c_2^*,$\Delta\gamma_2^*$

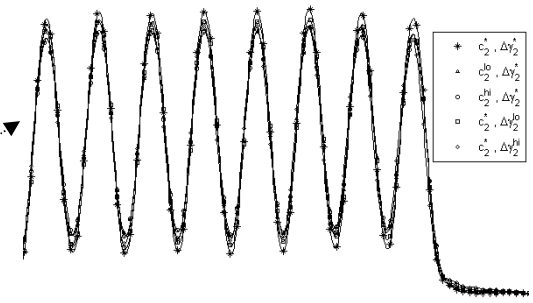

Fig. 7. Profiles of line-pair gauge using various geometry parameters for reconstruction

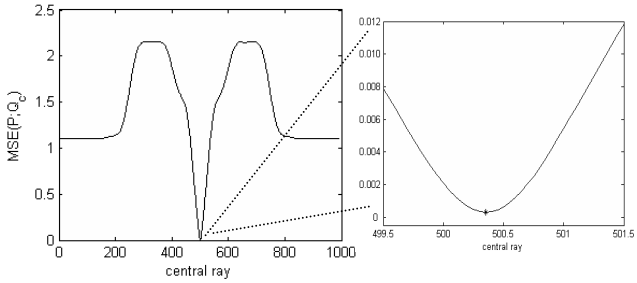

Fig. 5. MSE as a function of central ray

mean square error (MSE) and mean absolute error, as well as the negative of similarity measures such as mutual information (MI) and normalized mutual information (NMI) [4]. In principle, geometric calibration could work for any of these measures. In our experiments, however, MI and NMI proved to be poor choices due to slow speed, a nuisance parameter for histogram bin size, and no real benefit since P and Q have similar statistics. The fastest and most accurate results were achieved using MSE:

$$D_{MSE}(P;Q_\Theta) = \sum_{i,k}\left[P(i,k) - Q_\Theta(i,k)\right]^2 \qquad (12)$$

To perform the search in (11), one can choose from a number of off-the-shelf numerical optimization methods such as those in [5]. Gradient-based methods which work by evaluating $\nabla_\Theta D$ can offer quick convergence, but the exact updates are dependent on the choices of interpolation method and difference measure – for some choices, the updates can become rather intractable. Search methods requiring only evaluations of D, on the other hand, allow one to easily adjust the interpolation method or difference measure without modifying the search updates, and can still provide good speed. In experiments, a successive parabolic approximation algorithm[6] was able to perform c-ray measurement to within 0.1 channels using typically 6-15 evaluations of D. Different search methods in principle vary in their speed to convergence and region of convergence, but not in their accuracy – as long as they actually do converge to the right neighborhood, any competent optimization method will return the same result to within an arbitrarily small tolerance. Therefore the experimental results in Section 4 will focus on the quality of the optima found, with little discussion of the specifics of the search algorithm.

4. EXPERIMENTAL RESULTS

In this Section, experimental results are given using the proposed framework. Section 4.1 demonstrates the method on real scan data, while Section 4.2 gives results for c-ray calibration accuracy and noise-immunity on simulated data.

Calibration was performed using the methods of [6] with a specified accuracy of 0.0001 rays for c, and 0.01% for $\Delta\gamma$. Experience dictates that for high-quality CT images, as a rough rule of thumb, c should be accurate to within 0.1-0.25 rays and $\Delta\gamma$ should be accurate to 0.1-1%. The tighter tolerances used in this paper are for academic understanding.

4.1. Calibration on Real Data

The first validation was performed on a custom CT scanner using a 6MV linear accelerator source. The detector was constructed with channels with 0.75mm apertures, arranged at a 1.5mm pitch on an arc focused on the source with a focal length of approximately 3.05m, giving a nominal value of $\Delta\gamma_{nom} = 0.028178°$. Figure 4 shows projection data from a scan of a composite test part with several line-pair gauges placed around it. Figure 5 shows D as a function of c, keeping $\Delta\gamma$ fixed at $\Delta\gamma_{nom}$. C-ray calibration is performed by finding the minimum of this function, which is at c_1^*=500.3535. C-ray+pitch calibration then found the values c_2^*=500.3526 and $\Delta\gamma_2^*$=0.028355. Figure 6 shows the reconstruction using these values. To evaluate the obtained results, the above reconstruction was compared with reconstructions using nearby values, $c_2^{hi,lo} = c_2^* \pm 0.4$ rays, and $\Delta\gamma_2^{hi,lo} = \Delta\gamma_2^* \pm 10\%$. If our calibration worked, we would expect the reconstructions using the suboptimal parameters to be blurrier than the reconstructions using (c_2^*,$\Delta\gamma_2^*$). Figure 7 shows the same profile through targeted reconstructions of one of the line-pair gauges, using the indicated parameters. One can see that (c_2^*,$\Delta\gamma_2^*$) gives a larger peak-to-peak amplitude than the nearby parameters, which evidently cause more blur in the image. Thus it appears that the proposed framework produces parameters

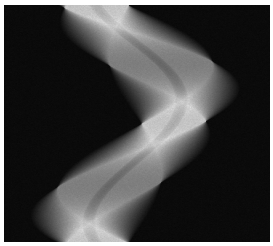

Fig. 8. Simulated projection data

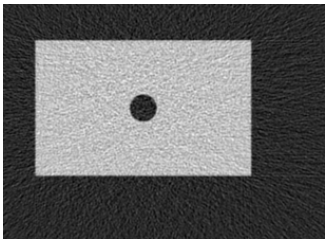

Fig. 9. Reconstruction of Fig. 8

Signal through air (each channel)		**Central Ray Measurement Error** (listed by percentile)				
photons	SNR	0% (best)	25%	50% (median)	75%	100% (worst)
10^5	316	0.000109	0.000994	0.00365	0.00578	0.00967
10^4	100	0.0000637	0.00166	0.00421	0.0053	0.00979
10^3	31.6	0.000766	0.0356	0.0745	0.106	0.135
10^2	10	0.000645	0.0896	0.244	0.337	0.449

Table 1. Central ray measurement accuracy from simulated noisy data

which are locally (and presumably globally) optimal. Note that it took a hefty perturbation of 10% on $\Delta\gamma$ to see this increase in blur. Smaller perturbations produced a negligible blur, but small errors in $\Delta\gamma$ can be observed to produce slight large-scale geometric warpings of the image.

4.2. Calibration on Synthetic Data

The next test was to simulate known geometry values, then test the algorithm's ability to recover these values in the presence of noise. The simulated geometry had 1024 detector channels with 0.8mm apertures arranged at a 1mm pitch along an arc with focal length 1300mm, focused on an x-ray source with a 1mm spot size. The rotation axis was 735 mm in front of the source, and the object was an 80mm×50mm box with a 10mm hole in its center. The box had attenuation equivalent to Aluminum for a 300keV monochromatic beam, was placed with its center 36mm away from the rotation axis, and was scanned using 1000 views per revolution. Data sets were generated for several different flux amounts, adding Gaussian noise to the pre-corrected projection data in order to model photon noise. For each flux amount, 50 different sets of projection data were generated, each with a different simulated central-ray value c_{sim}, the values ranging from 506 to 510. As an example, Figure 8 shows the projection data for 1000 photons per channel simulated with c_{sim}=507.1429, and Figure 9 shows the corresponding reconstruction. For this same data set, the proposed c-ray calibration returns c^*=507.2024, which agrees quite well with the simulated value. Table 1 shows the measurement accuracy $|c^*-c_{sim}|$ for all the different flux amounts – the indicated percentiles summarize the range of measurement errors seen over the 50 trials for each flux amount. We see that for high SNR ($\geq 10^4$ photons per channel), we in every case measured c to within $1/100^{th}$ of a channel – far better than we need. For a moderate SNR (10^3 photons per channel), we can measure c to a little worse than $1/10^{th}$ of a channel, still quite adequate for most imaging applications. For low SNR (100 photons per channel), the calibration result was always within ½ a channel, but only within our ideal ¼ channel half of the time.

5. CONCLUSIONS AND FUTURE DIRECTIONS

The proposed framework has a number of practical advantages in that it allows calibration from arbitrary objects, including calibration from the same scan data that will be fed to reconstruction. On real data, it found parameters that empirically seem to minimize reconstruction blur, and on synthetic data, it gave excellent results on high-SNR data, and still gave good results on noisy data. A future study could similarly quantify robustness to errors in the measurement of β, which occur due to mechanical practicalities. In this paper, we focused on global geometry parameters which affect all channel angles, though in the future, the proposed framework could be adapted to also include local parameters like polygonal module positions or even full-angle calibration. One major limitation, however, is that since the method relies on complementary rays, for a highly asymmetric detector configuration (such as [7]), local parameters may only be measured for those few channels whose complement actually exists. Nevertheless, the ability to calibrate geometry from scans of unknown objects, successfully demonstrated here, greatly simplifies the mechanical requirements for geometric CT calibration.

6. REFERENCES

[1] D.L. Parker, "Optimal short scan convolution reconstruction for fan beam CT," Med. Phys. vol 9 no 2, pp 254-257, 1982.

[2] J. Hsieh, *Computed Tomography: Principles, Design, Artifacts, and Recent Advances*, SPIE Press, Bellingham WA, 2003.

[3] G.K. Rohde, C.A. Berenstein, D.M. Healy Jr., "Measuring Image Similarity in the Presence of Noise," *Medical Imaging 2005: Image Processing*, ed. J.M. Fitzpatrick, J.M. Reinhart, Proceedings of SPIE, vol 5747, SPIE Press, Bellingham, WA, pp. 132-143, Feb 2005.

[4] J.P.W. Pluim, J.B.A. Maintz, and M.A. Viergever, "Mutual Information based registration of medical images: a survey," IEEE Trans. Medical Imaging, vol 22 no 8, pp. 986-1004, Aug, 2003.

[5] W. Press, B. Flannery, S. Teukolsky, and W. Vetterling, *Numerical Recipes in C: The Art of Scientific Computing*, Cambridge University Press, Cambridge, 1988.

[6] K.M. Holt, "Method and apparatus to facilitate determination of a parameter that corresponds to a scanning geometry characteristic," May 2006, US patent pending.

[7] G. Wang, "X-ray micro-CT with a displaced detector array," Med Phys. vol 29, no 7, pp 1634-1636, July 2002.